Research on QPSO algorithm for trajectory planning of FFSR general kinematics modeling

Huazhong Li*

Shenzhen Institute of Information Technology, Shenzhen, 518172, Guangdong, China

Abstract. Aiming at the optimal trajectory planning problem faced by free floating space robot (**FFSR**) in capturing non cooperative target (**NCT**) with unknown dynamic parameters, firstly, based on the unique intrinsic characteristics of **FFSR** in microgravity environment, a general **FFSR** kinematic model based on generalized velocity variables and an **NCT** dynamic model based on quaternion method are established. Secondly, the optimal criterion of **FFSR** trajectory planning and the parametric modeling method of **FFSR** manipulator joint trajectory based on sinusoidal function are studied; Finally, a **QPSO** algorithm for FFSR trajectory planning based on the optimal comprehensive index is proposed

Keywords: FFSR, NCT, Kinematic, Trajectory planning, QPSO.

1 Introduction

Free-Floating Space Robot (**FFSR)** is composed of a tracking satellite body and a mechanical arm mounted on it. It can fly or float freely in the universe and replace astronauts to complete **EVA** operation. In view of the importance of **FFSR** in future space operations, the optimal trajectory planning and control problem faced by **FFSR** capturing Non-Cooperative Target (**NCT)** has become one of the research focuses of scholars [1-5]. Many scholars put forward the trajectory planning scheme of **FFSR** capturing **NCT** from different angles. Most scholars regard **NCT** as a point target or a rigid body with known state and dynamic parameters, thus ignoring the complex dynamics and autonomous acquisition problems caused by the rolling state of **NCT** with unknown motion state and dynamic parameters.

Dubowsky et al. proposed to use disturbance diagram to express the influence of manipulator motion on spacecraft attitude [6]. Papadopoulos et al. used coordinate transformation to map nonholonomic constraints into a space that can simplify operation, avoiding the generation of dynamic singular points, and the planned trajectory is smooth and continuous [7]. Inaba et al. proposed a method for on orbit recognition and acquisition of **NCT** assuming that the shape, size and mass of the target are known [8]. M. D. Lichter et al. studied the recognition of **NCT**, and used laser imaging to estimate the shape, motion and related parameters of targets [9]. Z. Ma et al. proposed a trajectory iteration algorithm with minimum fuel consumption for the optimal control of the rendezvous between **FFSR** and

* Corresponding author: chinawwwsl@163.com

spatial rotating targets with known dynamic parameters [10]. F. Aghili et al. first studied the trajectory planning of **FFSR** capturing **NCT** without considering the conditional constraints of capture time, and then proposed a similar scheme to increase joint and speed constraints [11]. P. Singla et al. proposed the visual guidance method of **FFSR** automatic interception and berthing **NCT**, and proposed the adaptive control method of spacecraft interception and berthing according to the uncertainty of computer vision measurement [12]. Xu W F et al. designed a trajectory planning algorithm in cartesian coordinates by using the nonholonomic motion characteristics of **FFSR** system, and combined with particle swarm optimization (**PSO**) to search the optimal solution of the objective function [13]. Liu ZX et al. studied the trajectory optimization of the manipulator of **FFSR**. In order to make the attitude stability of **FFSR** system unaffected, a parametric trajectory planning method based on **PSO** is proposed [14]. Shi Zhong et al. proposed a nonholonomic motion planning method based on polynomial interpolation and **PSO** for **FFSR** trajectory planning [15]. Quantum-behaved particle swarm optimization(**QPSO**) is a very important branch in the field of cluster intelligence. **QPSO** algorithm has simple concept, less parameters, easy implementation and fast convergence speed. **QPSO** algorithm mainly adopts the superposition state characteristics and probability expression characteristics in quantum theory. Among them, the superposition state characteristics can make a single particle express more states and potentially increase the diversity of the population. The probability expression characteristic is to express the state of the particle with a certain probability, and the probability of the occurrence state is involved in the operation [16] [17] [18]. Shi Ye et al. transformed the nonholonomic cartesian path planning problem of **FFSR** system into the optimization problem of nonlinear system, and solved the nonlinear optimization problem by using **QPSO** algorithm, realizing the goal of nonholonomic path planning [19]. From the current research status, the problem of **FFSR** capturing **NCT** faces severe challenges and becomes the bottleneck of research in the research of basic theories and technologies such as **QPSO** optimal trajectory planning based on machine vision.

2 FFSR general kinematics modeling

The **FFSR** studied in this paper consists of $(n+1)$ connecting links L_i ($i=0\sim n$) connected by n number joints J_i （$i=1\sim n$）. The parameter symbols for connecting link i are agreed as follows. $\mathbf{r}_{c_i}\in\mathbf{R}^3$ represents the mass center vector of connecting link i. $\boldsymbol{\omega}_i=\dot{\mathbf{q}}_i\in\mathbf{R}^3$ represents the angular velocity vector of connecting link i. $\dot{\mathbf{r}}_{c_i}\in\mathbf{R}^3$ represents the velocity vector of the mass center C_i of the connecting link i. $\boldsymbol{\tau}_i\in\mathbf{R}^3$ represents the torque vector acting on C_i point on connecting link i. $\mathbf{f}_i\in\mathbf{R}^3$ represents the external force vector acting on C_i point on connecting link i. $\mathbf{I}_i\in\mathbf{R}^{3\times3}$ represents the inertia matrix of the connecting link i relative to the center of mass C_i. m_i represents the mass of connecting link i. The generalized velocity vector $\boldsymbol{\upsilon}_i\in\mathbf{R}^6$ of connecting link i is defined as equation (1).

$$\boldsymbol{\upsilon}_i=\left[\boldsymbol{\omega}_i,\quad \dot{\mathbf{r}}_{c_i}\right]^T \tag{1}$$

The generalized force vector $\mathbf{w}_i\in\mathbf{R}^6$ acting on the C_i point on the connecting link i

is defined as equation (2).

$$\mathbf{w}_i = [\boldsymbol{\tau}_i, \quad \mathbf{f}_i]^T \tag{2}$$

The generalized mass matrix $\mathbf{M}_i \in \mathbf{R}^{6\times6}$ of connecting link i is defined as equation (3).

$$\mathbf{M}_i = \begin{bmatrix} \mathbf{I}_i & \mathbf{0}_3 \\ \mathbf{0}_3 & \mathbf{m}_i \end{bmatrix} \tag{3}$$

Where, $\mathbf{0}_3$ is the zero matrix of $\mathbf{R}^{3\times3}$ space, $\mathbf{m}_i = m_i \mathbf{1}_3 \in \mathbf{R}^{3\times3}$, $\mathbf{1}_3 = diag(1,1,1) \in \mathbf{R}^{3\times3}$ is the identity matrix. The generalized momentum $\mathbf{p}_i \in \mathbf{R}^6$ of connecting link i is defined as equation (4).

$$\mathbf{p}_i = [\boldsymbol{\alpha}_i, \quad \mathbf{h}_i]^T \tag{4}$$

Where, $\boldsymbol{\alpha}_i \in \mathbf{R}^3$ represents the angular momentum vector $\mathbf{I}_i\boldsymbol{\omega}_i$ of the connecting link i around the center of mass C_i. $\mathbf{h}_i \in \mathbf{R}^3$ represents the linear momentum vector ($\mathbf{h}_i = m_i \dot{\mathbf{r}}_{c_i}$) of connecting link i. Using the generalized velocity $\boldsymbol{\upsilon}_i$ of the connecting link i defined by equation (1) and the generalized mass $\mathbf{M}_i$ defined by equation (3), the generalized momentum $\mathbf{p}_i$ of the connecting link i can be expressed as $\mathbf{p}_i = \mathbf{M}_i \boldsymbol{\upsilon}_i$. Considering the **FFSR** system composed of $n + 1$ links (including satellite body 0 and n links of manipulator), its $6(n + 1)$ dimensional generalized velocity vector and $6(n + 1) \times 6(n + 1)$ dimensional generalized mass matrix are defined as formula (5).

$$\boldsymbol{\upsilon} = [\boldsymbol{\upsilon}_S, \quad \boldsymbol{\upsilon}_1, \quad \cdots, \quad \boldsymbol{\upsilon}_n]^T, \quad \mathbf{M} = diag(\mathbf{M}_S, \mathbf{M}_1, \cdots, \mathbf{M}_n) \tag{5}$$

Where, $\boldsymbol{\upsilon}_S$ and $\mathbf{M}_S$ represent the generalized velocity vector and generalized mass matrix of the satellite body respectively. Therefore, the generalized total momentum $\mathbf{G} \in \mathbf{R}^6$ of **FFSR** system is defined as equation (6).

$$\mathbf{G} = [\mathbf{A}, \quad \mathbf{L}]^T \tag{6}$$

Where, $\mathbf{A} \equiv \sum_{i=0}^{n} \left(\mathbf{I}_i \boldsymbol{\omega}_i + \mathbf{r}_{c_i} \times m_i \dot{\mathbf{r}}_{c_i} \right) \in \mathbf{R}^{3\times1}$ and $\mathbf{L} = \sum_{i=0}^{n} \left(m_i \dot{\mathbf{r}}_{c_1} \right) \in \mathbf{R}^{3\times1}$ are the total angular momentum and total linear momentum of the fixed reference point relative to the inertial coordinate system $\boldsymbol{\Sigma}_I$ respectively.

$$K_i = \boldsymbol{\upsilon}_i^T \mathbf{M}_i \boldsymbol{\upsilon}_i / 2 \tag{7}$$

Where, $\boldsymbol{\upsilon}_i$ and $\mathbf{M}_i$ are defined by equations (1) and (3) respectively, and their physical meanings represent the generalized velocity vector and generalized mass matrix of connecting link i respectively.

$$\partial K_i / \partial \boldsymbol{\upsilon}_i = \mathbf{M}_i \boldsymbol{\upsilon}_i \tag{8}$$

Where, The physical meaning of term $\mathbf{M}_i \boldsymbol{\upsilon}_i$ on the right of equation (8) means that it is a $\mathbf{R}^6$ dimensional vector composed of the angular momentum and linear momentum of connecting link i around its center of mass C_i, representing the generalized total momentum (**GTM**) of connecting link i. The total kinetic energy K of the FFSR system composed of $\mathrm{n}+1$ connecting rods can be expressed as equation (9).

$$K = \sum_{i=0}^{n} \left(\boldsymbol{\upsilon}_i^T \mathbf{M}_i \boldsymbol{\upsilon}_i \right) / 2 = \boldsymbol{\upsilon}^T \mathbf{M} \boldsymbol{\upsilon} / 2 \tag{9}$$

Where, the physical meanings of $\boldsymbol{\upsilon}$ and $\mathbf{M}$ represent the generalized velocity vector and generalized mass matrix of **FFSR** system respectively. Applying the **GTM** concept of connecting link i to the whole **FFSR** system, the GTM for any p point of the system can be obtained.

$$\mathbf{G}_p = \partial K / \partial \boldsymbol{\upsilon}_p \tag{10}$$

Using the translation theorem and the axis theorem, the generalized total momentum (**GTM**) of FFSR system can be expressed as equation (11).

$$\mathbf{G} = \mathbf{C}_p \mathbf{G}_p \tag{11}$$

Where, $\mathbf{C}_p = \begin{bmatrix} \mathbf{1}_3 & \hat{\mathbf{r}}_{cp} \\ \mathbf{0}_3 & \mathbf{1}_3 \end{bmatrix} \in \mathbf{R}^{6\times 6}$, $\hat{\mathbf{r}}_{cp} \in \mathbf{R}^{3\times 3}$ represents the 3x3 cross product tensor of the centroid position vector $\mathbf{r}_{cp}$ of the **FFSR** system. Replace equation (9) with equation (10) to obtain equation (12).

$$\mathbf{G}_p = \left(\partial \boldsymbol{\upsilon} / \partial \boldsymbol{\upsilon}_p \right)^T \mathbf{M} \boldsymbol{\upsilon} \tag{12}$$

According to the kinematic constraint relationship of the connecting rod of FFSR system, the velocity vector can be expressed as equation (13).

$$\boldsymbol{\upsilon} = K_p \boldsymbol{\upsilon}_p + \boldsymbol{\upsilon}_J \tag{13}$$

Where, K_p is the $6(n+1)\times 6$ dimensional matrix related to $\boldsymbol{\upsilon}_p$. $\boldsymbol{\upsilon}_J$ represents the $6(n+1)$ dimensional vector of joint motion function. For the type of rotating joint, the expression (14) of $\partial \boldsymbol{\upsilon} / \partial \boldsymbol{\upsilon}_p$ term can be obtained from equation (13).

$$K_p = \partial \boldsymbol{\upsilon} / \partial \boldsymbol{\upsilon}_p \tag{14}$$

Replace (14) with (12) to obtain formula (15).

$$\mathbf{G}_p = K_p^T \mathbf{M} \boldsymbol{\upsilon} \tag{15}$$

Therefore, the generalized total momentum $\mathbf{G}$ of equation (11) can be derived from equations (13) and (15) to equation (16).

$$\mathbf{G} = \mathbf{C}_p \mathbf{G}_p = \mathbf{C}_p K_p^T \mathbf{M} \boldsymbol{\upsilon} = \mathbf{C}_p K_p^T \mathbf{M} \left(K_p \boldsymbol{\upsilon}_p + \boldsymbol{\upsilon}_J \right) \tag{16}$$

If the satellite motion is known, taking the satellite as the reference point, the angular velocity $\boldsymbol{\omega}_E$ and velocity $\dot{\mathbf{r}}_{c_E}$ of the end effector can be expressed as:

$$\boldsymbol{\omega}_E = \boldsymbol{\omega}_S + \sum_{i=1}^{n} \left(\dot{q}_i \mathbf{e}_i \right) \tag{17}$$

$$\dot{\mathbf{r}}_{c_E} = \dot{\mathbf{r}}_{c_0} + \boldsymbol{\omega}_S \times \boldsymbol{\rho}_S + \sum_{i=1}^{n} \left(\dot{q}_i \mathbf{e}_i \times \boldsymbol{\rho}_i \right) \tag{18}$$

Combining (17) and (18) to describe the generalized velocity vector of the manipulator end effector, the generalized velocity vector $\boldsymbol{\upsilon}_E$ of the FFSR system described in equation (13) can be expressed as:

$$\boldsymbol{\upsilon}_E = \mathbf{K}_S \boldsymbol{\upsilon}_S + \mathbf{K}_M \dot{\mathbf{Q}}_M \tag{19}$$

Where, $\boldsymbol{\upsilon}_S$ represents the generalized velocity vector of **FFSR** satellite base. $\mathbf{Q}_M = [q_1, \ \cdots, \ q_n]^T \in \mathbf{R}^n$ represents the configuration of **FFSR** manipulator. $\dot{\mathbf{Q}}_M = [\dot{q}_1, \ \cdots, \ \dot{q}_n]^T \in \mathbf{R}^n$ represents the joint angular velocity vector of FFSR manipulator. The scalar q_i （$i = 1, \cdots, n$） is the rotational angular displacement of the joint. Scalar $\dot{q}_i$ （$i = 1, \cdots, n$） is the rotational angular velocity of joint J_i. $\mathbf{K}_S = \begin{bmatrix} \mathbf{1}_3 & \mathbf{0}_3 \\ -\mathbf{p}_S \times \mathbf{1} & \mathbf{1}_3 \end{bmatrix} \in \mathbf{R}^{6\times6}$ and $\mathbf{K}_M = \begin{bmatrix} \mathbf{e}_1 & \cdots & \mathbf{e}_n \\ \mathbf{e}_1 \times \mathbf{p}_1 & \cdots & \mathbf{e}_n \times \mathbf{p}_n \end{bmatrix} \in \mathbf{R}^{6\times n}$ represent the generalized matrix coefficients of **FFSR** satellite and **FFSR** manipulator respectively. Comparing equation (13) with equation (19), we can see $\boldsymbol{\upsilon}_J = \mathbf{K}_M \dot{\mathbf{Q}}_M$. Using equation (19), the generalized total momentum $\mathbf{G}$ expressed by equation (16) can be obtained.

$$\mathbf{G} = \mathbf{C}_S \left(\mathbf{I}_S \boldsymbol{\upsilon}_S + \mathbf{I}_M \dot{\mathbf{Q}}_M \right) \tag{20}$$

Where, $\mathbf{I}_S = \mathbf{K}_S^T \mathbf{M} \mathbf{K}_S \in \mathbf{R}^{6\times6}$ and $\mathbf{I}_M = \mathbf{K}_S^T \mathbf{M} \mathbf{K}_M \in \mathbf{R}^{6\times n}$ represent the symmetrical inertia matrix of the satellite body and the inertia matrix of the manipulator respectively. The definition of $\mathbf{C}_S$ is related to the satellite base position vector $\mathbf{r}_{c_0}$. $\mathbf{e}_i$ is a 3-dimensional unit vector parallel to the rotation axis of joint i. Equation (19) describes the relationship between the generalized velocity vector $\boldsymbol{\upsilon}_S$ of the satellite base and the angular velocity vector $\dot{\mathbf{Q}}_M$ of the manipulator joint. In order to facilitate the kinematic analysis of **FFSR**, it is expected to obtain the relationship between the generalized velocity vector $\boldsymbol{\upsilon}_E$ of the manipulator end effector and the joint angular velocity vector $\dot{\mathbf{Q}}_M$. For this purpose, considering **FFSR** kinematic constraints, equation (21) can be obtained.

$$\boldsymbol{\upsilon}_E = \mathbf{J}_S\boldsymbol{\upsilon}_S + \mathbf{J}_M\dot{\mathbf{Q}}_M \tag{21}$$

Where, $\boldsymbol{\upsilon}_E = [\boldsymbol{\omega}_E \quad \dot{\mathbf{r}}_{c_E}]^T$ is the generalized velocity vector of the end effector. $\boldsymbol{\omega}_E$ is the angular velocity of the end effector. $\boldsymbol{\omega}_E$ is the velocity vector at point E on the end effector. $\dot{\mathbf{r}}_{c_E}$ is the velocity vector at point E on the end effector. $\mathbf{J}_S \in \mathbf{R}^{6\times 6}$ and $\mathbf{J}_M \in \mathbf{R}^{6\times n}$ represent the jacobian matrix of satellite and **FFSR** manipulator respectively.

$$\boldsymbol{\upsilon}_E = \mathbf{J}^*\dot{\mathbf{Q}}_M + \mathbf{H}^*\mathbf{G} \tag{22}$$

Where, $\mathbf{J}^* = \mathbf{J}_M - \mathbf{J}_S\mathbf{I}_S^{-1}\mathbf{I}_M \in \mathbf{R}^{6\times n}$, $\mathbf{H}^* = \mathbf{J}_S\mathbf{I}_S^{-1}\mathbf{C}_S^{-1} \in \mathbf{R}^{6\times 6}$. Because $\mathbf{I}_S$ is a symmetric positive definite matrix, its inverse matrix $\mathbf{I}_S^{-1}$ exists. According to the definition of $\mathbf{C}_S$, it can be seen that its inverse $\mathbf{C}_S^{-1}$ exists. $\mathbf{J}^*$ is the so-called generalized Jacobian matrix(**GJM**) of FFSR. If the motion of the end effector is known, taking the end effector as the reference point, the generalized velocity vector of the FFSR system described in equation (13) can be expressed as:

$$\boldsymbol{\upsilon} = \mathbf{K}_E\boldsymbol{\upsilon}_E + \hat{\mathbf{K}}_M\dot{\mathbf{Q}}_M \tag{23}$$

Where, $\mathbf{K}_E \in \mathbf{R}^{6\times 6}$, $\hat{\mathbf{K}}_M \in \mathbf{R}^{6(n+1)\times n}$. $\boldsymbol{\upsilon}_E$ is determined by equation (22). The generalized total momentum with the end effector as the reference point can be expressed as:

$$\mathbf{G} = \mathbf{C}_E\left(\mathbf{I}_E\boldsymbol{\upsilon}_E + \hat{\mathbf{I}}_M\dot{\mathbf{Q}}\right) \tag{24}$$

Where, $\mathbf{C}_E \in \mathbf{R}^{6\times 6}$ is related to $\mathbf{r}_{c_E}$. $\mathbf{I}_E = \mathbf{K}_E^T\mathbf{M}\mathbf{K}_E \in \mathbf{R}^{6\times 6}$ and $\hat{\mathbf{I}}_M = \mathbf{K}_E^T\mathbf{M}\hat{\mathbf{K}}_M \in \mathbf{R}^{6\times n}$. Thus, the kinematic model between the generalized motion velocity vector of the end effector and the joint velocity vector can be derived as follows:

$$\boldsymbol{\upsilon}_E = \mathbf{J}\dot{\mathbf{Q}}_M + \mathbf{H}\mathbf{G} \tag{25}$$

Where, $\mathbf{J} = \mathbf{I}_E^{-1}\hat{\mathbf{I}}_M \in \mathbf{R}^{6\times n}$, $\mathbf{H} = \mathbf{I}_E^{-1}\mathbf{C}_E^{-1} \in \mathbf{R}^{6\times 6}$. Because $\mathbf{I}_E$ is a symmetric positive definite matrix, its inverse $\mathbf{I}_E^{-1}$ obviously exists. Comparing equations (22) and (25), it is obvious that the expression of matrix $\mathbf{J}$ is much simpler than **GJM** matrix $\mathbf{J}^*$. The research shows that the calculation of velocity decomposition control with end effector as reference point is less. Considering that **FFSR** system satisfies the law of conservation of momentum (Conservation of linear momentum and conservation of angular momentum), that is, $\mathbf{G}$ = constant; And the initial state is static, $\mathbf{G} = 0$, then the kinematic model (22) with the satellite as the reference point is simplified into:

$$\boldsymbol{\upsilon}_E = \mathbf{J}^*\dot{\mathbf{Q}}_M \tag{26}$$

The kinematic model (25) with the end effector as the reference point is simplified into:

$$\boldsymbol{\upsilon}_E = \mathbf{J}\dot{\mathbf{Q}}_M \tag{27}$$

Obviously, the kinematics model with the end effector as the reference point can more effectively deal with the forward kinematics and inverse kinematics control problems of FFSR. For inverse kinematics, the joint angle $\mathbf{Q}_M$ of the manipulator can be calculated according to the given generalized velocity $\boldsymbol{\upsilon}_E$ of the end effector.

When n = 6, the matrix $\mathbf{J}^*$ or $\mathbf{J} \in \mathbf{R}^{6\times 6}$, if the **FFSR** is of nonsingular configuration, the inverse of $\mathbf{J}^*$ or $\mathbf{J}$ exists, so that $\dot{\mathbf{Q}}_M$ can be obtained, and then $\mathbf{Q}_M$ can be obtained by integration.

$$\dot{\mathbf{Q}}_M = (\mathbf{J}^*)^{-1}\boldsymbol{\upsilon}_E \text{ or } \dot{\mathbf{Q}}_M = (\mathbf{J})^{-1}\boldsymbol{\upsilon}_E \tag{28}$$

When n > 6, **FFSR** system is redundantly driven, (24) is an underdetermined system with n unknown variables and 6 linear equations, which can not uniquely determine $\dot{\mathbf{Q}}_M$; In this case, the optimization method can be used to solve the $\dot{\mathbf{Q}}_M$ value satisfying the constraint relationship of equation (24), so as to obtain:

$$\dot{\mathbf{Q}}_M = (\mathbf{J}^*)^{+}\boldsymbol{\upsilon}_E \text{ or } \dot{\mathbf{Q}}_M = (\mathbf{J})^{+}\boldsymbol{\upsilon}_E \tag{29}$$

It minimizes $\dot{\mathbf{Q}}_M^T\dot{\mathbf{Q}}_M/2$. $(\mathbf{J}^\times)^+$ is defined as the pseudo inverse matrix of $\mathbf{J}^\times$ ($\mathbf{J}^\times$ represents $\mathbf{J}^*$ or $\mathbf{J}$) as:

$$(\mathbf{J}^\times)^+ = (\mathbf{J}^\times)^T\left(\mathbf{J}_E(\mathbf{J}^\times)^T\right)^{-1} \tag{30}$$

3 NCT dynamic model based on quaternion method

Based on the theory of optimal control and estimation, this paper proposes an **FFSR** trajectory planning based on machine vision to intercept **NCT** with unknown dynamic parameters. The **QPSO** optimal trajectory control diagram of **NCT** captured by machine vision **FFSR** is shown in Figure 1. Its main idea is based on the "prediction planning control" method.

The extended Kalman filter (**EKF**) is used to obtain the reliable estimation of **NCT** motion state and dynamic parameters according to the noisy **NCT** measurement data collected by machine vision, so as to make the system converge as soon as possible, so as to reliably predict the **NCT** motion, and detect the convergence of the system by monitoring the covariance matrix of **EKF**. In order to avoid the huge impact force generated when **FFSR** captures **NCT**, it is necessary to establish an effective collision dynamics model. During the collision between **FFSR** and **NCT**, **FFSR** and **NCT** can be studied as a complete multi rigid body system. At this time, the collision force between **FFSR** and **NCT** can be regarded as internal force. In the microgravity environment, the linear momentum conservation, angular momentum conservation and energy conservation of the whole system meet the collision impulse theorem (collectively referred to as physical constraints). In addition, certain geometric constraints must be met during collision. The key problem is how to establish an effective model of **FFSR** collision dynamics in microgravity environment under physical and geometric constraints such as collision impulse theorem. Therefore, a dynamic model of

NCT based on quaternion method is established in this paper. Let the quaternion $\mathbf{q}$ represent the rotation of the **NCT** and $\boldsymbol{\omega}$ represent the angular velocity of the **NCT**, then the relationship between the derivative of the quaternion $\mathbf{q}$ to time and the angular velocity $\boldsymbol{\omega}$ can be described as equation (31)

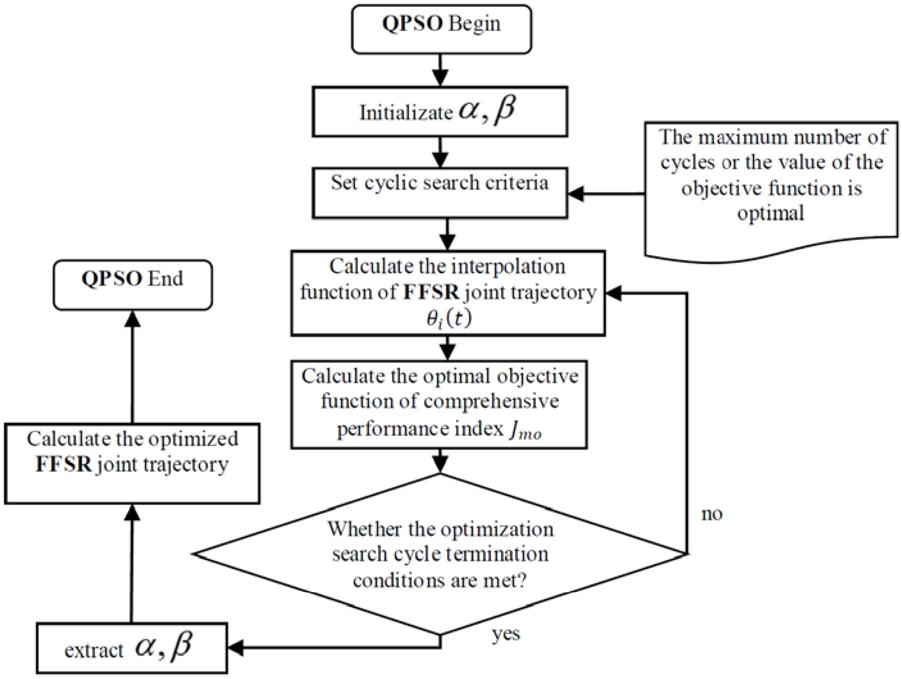

Fig. 1. QPSO optimal trajectory control diagram based on machine vision **FFSR** capturing **NCT**.

$$\dot{\mathbf{q}} = \frac{1}{2}\Omega(\boldsymbol{\omega})\mathbf{q} \tag{31}$$

Where, $\Omega(\omega)=\begin{bmatrix} -[\omega\times] & \omega \\ -\omega^T & 0 \end{bmatrix}$. Define the quaternion product operation $\otimes$ acting on the quaternion $\mathbf{q}$ as equation (32):

$$\mathbf{q}\otimes \equiv q_0\mathbf{1}_4 + \boldsymbol{\Omega}(\mathbf{q}_v) \tag{32}$$

Where, $\mathbf{q}_v$ is the vector part of the quaternion, q_0 is the scalar part, so, $\mathbf{q} = \begin{bmatrix}\mathbf{q}_v^T & q_0^T\end{bmatrix}^T$. Thus, the product $\mathbf{q}_1 \otimes \mathbf{q}_2$ of the two quaternions corresponds to the rotation matrix $\mathbf{A}(\mathbf{q}_2)\mathbf{A}(\mathbf{q}_1)$, and the relationship between the rotation matrix $\mathbf{A}(\mathbf{q})$ and the corresponding quaternion is as follows (33):

$$\mathbf{A}(\mathbf{q}) = (2q_0^2 - 1)\mathbf{1}_3 + 2q_0[q_v\times] + 2\mathbf{q}_v\mathbf{q}_v^T \tag{33}$$

Therefore, the dynamic equation of **NCT** rotation can be described as Euler equation in the form of inertial parameters. According to this equation, based on the robot vision data, the extended Kalman filter (**EKF**) can be used to estimate the main inertial parameters of **NCT**.

4 Trajectory planning QPSO algorithm

This paper presents a **QPSO** algorithm for **FFSR** trajectory planning based on the optimal comprehensive index.

4.1 Determine the optimal criterion of FFSR trajectory planning

The commonly used optimization criteria in **FFSR** trajectory planning are: time optimal trajectory planning, energy optimal trajectory planning, impact optimal trajectory planning and comprehensive optimal trajectory planning. In this paper, a comprehensive index optimization criterion based on **FFSR** is proposed to minimize the attitude disturbance of satellite base and meet the constraints of satellite base attitude variation range, joint angular velocity and angular acceleration.

4.1.1 Minimum objective function of satellite base attitude disturbance based on FFSR

In order to minimize the base attitude disturbance of **FFSR** manipulator, the goal of **FFSR** joint trajectory planning is to plan the movement of each joint angle of **FFSR** manipulator to meet the constraints of the following equations (34) ~ (36), and minimize the change of base attitude of **FFSR** satellite after the movement.

$$q_i(t_0) = q_{i0},\ \dot{q}_i(t_0) = \ddot{q}_i(t_0) = 0 \tag{34}$$

$$q_i(t_f) = q_{id},\ \dot{q}_i(t_f) = \ddot{q}_i(t_f) = 0\ \ (i = 1,2,\cdots,n) \tag{35}$$

$$q_{iMin} \le q_i(t) \le q_{iMax},\ |\dot{q}_i(t)| \le \dot{q}_{iL},\ |\ddot{q}_i(t)| \le \ddot{q}_{iL} \tag{36}$$

Where, q_{i0} and q_{id} are the initial angle and expected angle values of the i joint angle respectively. q_{iMin}, q_{iMax}, $\dot{q}_{iL}$ and $\ddot{q}_{iL}$ are the ranges of minimum joint angle, maximum joint angle, angular velocity and angular acceleration of the manipulator respectively. When the joint angular velocity and angular acceleration of **FFSR** manipulator are not limited, the goal of joint trajectory planning can be expressed as:

$$\boldsymbol{\Omega}_m(t_f) = \Omega_{md},\ \|\boldsymbol{\Phi}_s(t_f) - \boldsymbol{\Phi}_s(t_0)\| = \min \tag{37}$$

Where, $\boldsymbol{\Omega}_{md}$ is the expected joint angle of FFSR manipulator, and $\boldsymbol{\Phi}_s$ is the attitude angle of FFSR satellite base.

According to equation (37), the objective function of manipulator trajectory planning problem with minimum attitude disturbance of **FFSR** satellite base can be obtained, as shown in equation (38):

$$J_1 = \|\delta\boldsymbol{\Phi}_s\|/k_\Phi \tag{38}$$

Where, $\|\delta\boldsymbol{\Phi}_s\| = \sqrt{\delta\boldsymbol{\Phi}_s^T\delta\boldsymbol{\Phi}_s}$ represents the norm of the difference between the attitude angle at the termination time t_f of the satellite base and the attitude angle at the initial time of the satellite base. k_Φ is the weight coefficient, which is determined according to the accuracy requirements of trajectory planning. Different accuracy requirements only need to adjust k_{Φ}, and the objective function $J_1 \le 1$ means that the objective function has met the accuracy requirements.

4.1.2 Objective function considering joint angular velocity and acceleration constraints

Considering the ability of the executive device of the actual **FFSR** manipulator system, in order to ensure the stability and reliability of the operation of the **FFSR** manipulator, the angular velocity and angular acceleration of each joint angle of the **FFSR** manipulator must be limited within a certain range. It is necessary to study the description of the objective function when the joint angular velocity and angular acceleration are limited [20]. Here, the joint angular velocity and angular acceleration cost functions $J_{\dot{\Omega}_m}$ and $J_{\ddot{\Omega}_m}$ are introduced, as shown in equation (39).

$$J_{\dot{\Omega}_m} = \sum_{i=1}^{n} J_{\dot{q}_i}\ ,\ \ J_{\ddot{\Omega}_m} = \sum_{i=1}^{n} J_{\ddot{q}_i} \tag{39}$$

Where, When $\dot{q}_{iMax} \le \dot{q}_{iL}$, $J_{\dot{q}_i} = 0$. When $\dot{q}_{iMax} > \dot{q}_{iL}$, $J_{\dot{q}_i} = (\dot{q}_{iMax} - \dot{q}_{iL})/\dot{q}_{iL}$ .When $\ddot{q}_{iMax} \le \ddot{q}_{iL}$, $J_{\ddot{q}_i} = 0$. When $\ddot{q}_{iMax} > \ddot{q}_{iL}$, $J_{\ddot{q}_i} = (\ddot{q}_{iMax} - \ddot{q}_{iL})/\ddot{q}_{iL}$. $\dot{q}_{iMax}$ and $\ddot{q}_{iMax}$ are the maximum values of joint angular velocity and angular acceleration of the i joint in $[t_0, t_f]$ time respectively.

$$J_2 = J_{\dot{\Omega}_m}/k_{\dot{\Omega}_m} + J_{\ddot{\Omega}_m}/k_{\ddot{\Omega}_m} \tag{40}$$

Where, $k_{\dot{\Omega}_m}$ and $k_{\ddot{\Omega}_m}$ are the weight coefficients of acceleration constraint and angular acceleration constraint.

*4.1.3 Objective function considering the attitude range constraint of **FFSR** satellite base*

Considering that in practice, in order to ensure the normal operation of FFSR satellite, the attitude change of FFSR satellite base is required to be limited within a certain range. Therefore, it is necessary to define the following objective function to restrict the change range of satellite base attitude during the movement of FFSR manipulator:

$$J_3 = J_{\delta\boldsymbol{\Phi}_s}/k_{\delta\boldsymbol{\Phi}_s} \tag{41}$$

Where, $k_{\delta\Phi_s}$ is the attitude angle constraint weight coefficient. $J_{\delta\boldsymbol{\Phi}_s} = J_{\delta\Phi_{s\alpha}} + J_{\delta\Phi_{s\beta}} + J_{\delta\Phi_{s\gamma}}$.

When $\delta\Phi_{s\alpha M} \le \delta\Phi_{s\alpha L}$, $J_{\delta\Phi_{s\alpha}} = 0$. When $\delta\Phi_{s\alpha M} > \delta\Phi_{s\alpha L}$, $J_{\delta\Phi_{s\alpha}} = (\delta\Phi_{s\alpha M} - \delta\Phi_{s\alpha L})/\delta\Phi_{s\alpha L}$.Where,$\delta\Phi_{s\alpha M}$ is the maximum rotation angle of the base around the z axis in time $[t_0,\ t_f]$. $\delta\Phi_{s\alpha L}$ is the threshold value of the rotation angle of the base around the z axis. When $\delta\Phi_{s\beta M} \le \delta\Phi_{s\beta L}$, $J_{\delta\Phi_{s\beta}} = 0$. When $\delta\Phi_{s\beta M} > \delta\Phi_{s\beta L}$, $J_{\delta\Phi_{s\beta}} = (\delta\Phi_{s\beta M} - \delta\Phi_{s\beta L})/\delta\Phi_{s\beta L}$. Where, $\delta\Phi_{s\beta M}$ is the maximum value of the rotation angle of the base around the x axis in time $[t_0,\ t_f]$. $\delta\Phi_{s\beta L}$ is the threshold value of the rotation angle of the base around the x axis.

When $\delta\Phi_{s\gamma M} \le \delta\Phi_{s\gamma L}$, $J_{\delta\Phi_{s\gamma}} = 0$. When $\delta\Phi_{s\gamma M} > \delta\Phi_{s\gamma L}$, $J_{\delta\Phi_{s\gamma}} = (\delta\Phi_{s\gamma M} - \delta\Phi_{s\gamma L})/\delta\Phi_{s\gamma L}$. Where, $\delta\Phi_{s\gamma M}$ is the maximum value of the rotation angle of the base around y in time $[t_0,\ t_f]$. $\delta\Phi_{s\gamma L}$ is the threshold value of the rotation angle of the base around the y axis. Similarly, the same form of $J_{\delta\Phi_{s\beta}}$ and $J_{\delta\Phi_{s\gamma}}$ can be obtained.

*4.1.4 The minimum objective function considering the end position error of **FFSR** manipulator and the attitude error of satellite base.*

$$J_4 = \|\delta q\|/k_q + \|\delta p_e\|/k_p \tag{42}$$

Where, $\delta \boldsymbol{p}_e$ is the end position error of FFSR manipulator. $\delta\mathbf{q} = \eta_f q_d - \eta_d q_f - \tilde{q}_f q_d$ is the quaternion error of FFSR satellite base attitude (difference between final value $\{\eta_f, q_f\}$ and expected value $\{\eta_d, q_d\}$). Here, the norm $\|x\| = \mathrm{sqrt}(x^T x)$, k_q and k_p are weighting coefficients.

4.1.5 Optimal objective function of comprehensive index

According to the above analysis, considering the minimum attitude disturbance of satellite base and the minimum position error of manipulator end based on **FFSR**, and meeting the constraints of satellite base attitude variation range, joint angular velocity and angular acceleration, the optimal objective function of the comprehensive index is:

$$J_{mo} = \|\delta\Phi_s\|/k_\Phi + J_{\dot{\Omega}_m}/k_{\dot{\Omega}_m} + J_{\ddot{\Omega}_m}/k_{\ddot{\Omega}_m} + J_{\delta\Phi_s}/k_{\delta\Phi_s} + \|\delta q\|/k_q + \|\delta p_e\|/k_p \tag{43}$$

4.2 Parametric modeling of joint trajectory

In order to effectively and directly constrain the range of joint angles of **FFSR** manipulator and ensure the good smoothness of joint motion, this paper uses sinusoidal function to parameterize the joint function. In order to ensure the smoothness of the motion of **FFSR** manipulator at the initial time and termination time, the initial and termination states of the joint are usually required to meet the following constraint equations:

$$\mathbf{\Theta}(t_0) = \mathbf{\Theta_0},\ \dot{\mathbf{\Theta}}(t_0) = 0,\ \ddot{\Theta}(t_0) = 0,\ \dot{\mathbf{\Theta}}(t_f) = 0,\ \ddot{\mathbf{\Theta}}(t_f) = 0 \tag{44}$$

In addition, the range of motion of the joint angle of the **FFSR** manipulator is limited by the mechanical structure and meets the following conditions:

$$\theta_{imin} \le \theta_i(t) \le \theta_{imax},\ \ \mathrm{i} = 1,2,\cdots,\mathrm{n} \tag{45}$$

Where, θ_{imin} and θ_{imax} are the minimum and maximum values of joint i, respectively.

$$\theta_i(t) = \Delta_{i1} sin\left(\sum_{j=0}^{7} a_{ij} t^j\right) + \Delta_{i2} \tag{46}$$

Where, a_{i0}～a_{i7} is a pending parameter. Δ_{i1} and Δ_{i2} are determined according to the range of joint angle.

$$\Delta_{i1} = (\theta_{imax} - \theta_{imin})/2, \Delta_{i2} = (\theta_{imax} + \theta_{imin})/2 \tag{47}$$

Find the first and second derivatives of equation (46), then the joint angular velocity and angular acceleration of $\theta_i \in (\theta_{imin}, \theta_{imax})$ are guaranteed to be:

$$\dot{\theta}_i(\mathrm{t}) = \Delta_{i1} cos\left(\sum_{j=0}^{7}\left(a_{ij} t^j\right)\right)\left(\sum_{j=1}^{7}\left(j a_{ij} t^{(j-1)}\right)\right) \tag{48}$$

$$\ddot{\theta}_i(t) = -\Delta_{i1} sin\left(\sum_{j=0}^{7}\left(a_{ij} t^j\right)\right)\left(\sum_{j=1}^{7}\left(j a_{ij} t^{(j-1)}\right)\right)^2 + \Delta_{i1} cos\left(\sum_{j=0}^{7}\left(a_{ij} t^j\right)\right)\left(\sum_{j=7}^{2}\left((j)(j-1)\left(a_{ij} t^{(j-2)}\right)\right)\right) \tag{49}$$

The constraint conditions to make the joint angle and base attitude of **FFSR** manipulator reach the desired value at the same time are:

$$\boldsymbol{\Theta}(t_f) = \boldsymbol{\Theta_d} \tag{50}$$

Substituting equations (44) and (50) into equations (46) to (49) can obtain:

$$a_{i0} = \arcsin[(\theta_{i0} - \Delta_{i2})/\Delta_{i1}], a_{i1} = a_{i2} = 0 \tag{51}$$

$$a_{i3} = 10\big(arcsin((q_{id} - \Delta_{i2})/\Delta_{i1}) - arcsin((q_{is} - \Delta_{i2})/\Delta_{i1})\big)/t_f^3 - 3a_{i7}t_f^4 - a_{i6}t_f^3 \tag{52}$$

$$a_{i4} = 15\big(arcsin((q_{id} - \Delta_{i2})/\Delta_{i1}) - arcsin((q_{is} - \Delta_{i2})/\Delta_{i1})\big)/t_f^4 + 8a_{i7}t_f^3 + 3a_{i6}t_f^3 \tag{53}$$

$$a_{i5} = 6\big(arcsin((q_{id} - \Delta_{i2})/\Delta_{i1}) - arcsin((q_{is} - \Delta_{i2})/\Delta_{i1})\big)/t_f^5 - 6a_{i7}t_f^2 - 3a_{i6}t_f \tag{54}$$

Where, θ_{id} is the desired angle of the **FFSR** manipulator joint i. From equations (51) ~ (54), it can be seen that after the joint angle function of **FFSR** manipulator is parameterized, each joint function contains only two unknown parameters a_{i6} and a_{i7}. Therefore, for the **FFSR** manipulator with n joints, if the unknown parameter matrix $\mathbf{a}\epsilon\boldsymbol{R}^{2\times n}$ is determined, the joint trajectory of the **FFSR** manipulator can be uniquely determined, where the matrix **a** is:

$$\mathbf{a} = \begin{bmatrix} a_{16} & a_{26} & \cdots & a_{n6} \\ a_{17} & a_{27} & \cdots & a_{n7} \end{bmatrix} \tag{55}$$

Therefore, the optimal trajectory planning problem of **FFSR** manipulator studied in this paper can be transformed into: by solving the unknown parameter matrix **a** defined in equation (55), the optimal objective function J_{mo} of the comprehensive index described in equation (43) can be minimized.

4.3 Establish the mathematical model of FFSR optimal trajectory planning

The design idea of optimal trajectory planning of **FFSR** manipulator based on **QPSO** is described as follows. For **FFSR** manipulator with n joints, it is necessary to plan n joint angle trajectories at the same time. Each joint angle trajectory is uniquely determined by a set of (α_{id} 、 β_{id}) through parameterized sinusoidal function. The essence of optimization of joint space trajectory planning of FFSR manipulator is to find the optimal (α 、 β) combination.Therefore, the position x_j of the particle can be represented by the corresponding (α_i 、 β_i) combination, that is, $\mathbf{x}_i = \begin{bmatrix} a_{i1} & a_{i2} & \cdots & a_{in} \\ \beta_{i1} & \beta_{i2} & \cdots & \beta_{in} \end{bmatrix}^T$, and its search flow chart is shown in Fig. 2.

Let the number of particles be n, the number of iterations be K, and the maximum number of iterations be $\mathrm{N_{max}}$, the main steps of **QPSO** algorithm are described as follows.

Step 1 First, the initial position $\mathrm{X_i}(0) = \mathbf{a^i} = \begin{bmatrix} a_{16}^i & a_{26}^i & \cdots & a_{n6}^i \\ a_{17}^i & a_{27}^i & \cdots & a_{n7}^i \end{bmatrix} \epsilon R^{2\times n}(\mathrm{i} = 1,2,\cdots,\mathrm{N})$ of **N** particles is initialized randomly. Make the current best position of each particle $\mathrm{P_i}(0) = \mathrm{X_i}(0)$. The global best position is $\mathrm{P_g}(0) = \max\{\mathrm{X_0}(0), \mathrm{X_1}(0), \cdots, \mathrm{X_N}(0)\}$.

Step 2 According to equations (46), (48) and (49), the trajectory interpolation functions such as joint angle $\theta_i(t)$, joint angular velocity $\dot{\theta}_i(\mathrm{t})$ and joint angular acceleration $\ddot{\theta}_i(t)$ of FFSR manipulator are calculated.

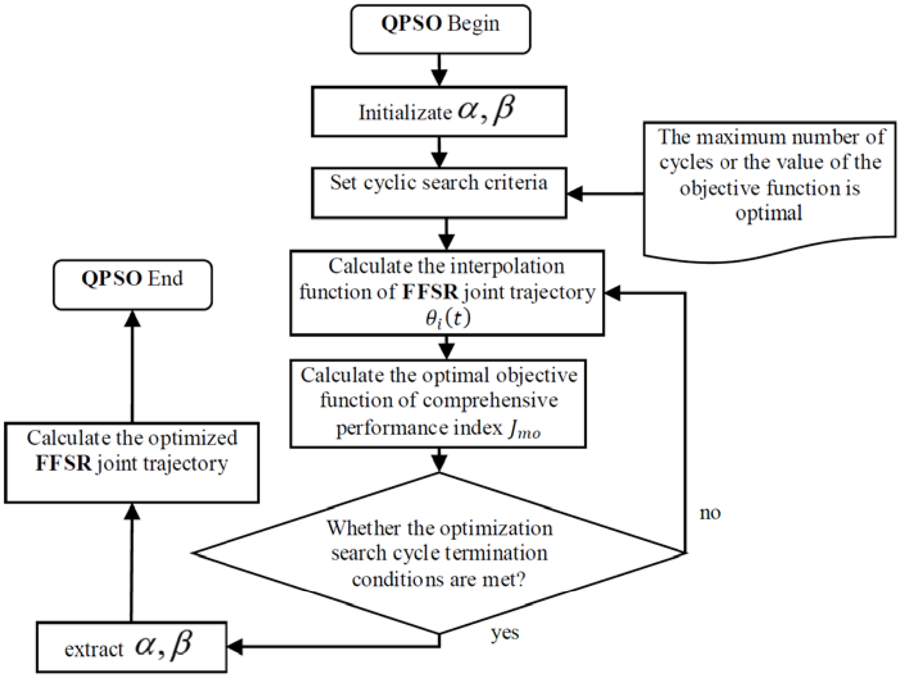

Fig. 2. Trajectory planning flow chart of **FFSR** manipulator based on **QPSO.**

Step 3 Calculate the fitness function (or objective function) $\mathrm{F}_i(k)$ of each particle by formula (43): $\mathrm{F}_i(k)$: $\mathrm{F}_i(k) = \mathrm{J}_{mo}(a^i(k))$, $\mathrm{i} = 1,2,\cdots,\mathrm{N}$.

Step 4 Calculate the new local optimal position $P_i(\mathrm{t}+1)$ of each particle: $P_i(\mathrm{t}+1) = \begin{cases} P_i(t), \mathrm{J}_{mo}(P_i(t)) \le \mathrm{J}_{mo}(X_i(t+1)) \\ X_i(t), \mathrm{J}_{mo}(P_i(t)) > \mathrm{J}_{mo}(X_i(t+1)) \end{cases}$.

Step 5 Update the global optimal location: $\mathrm{P_g}(\mathrm{t}+1) = \max\{\mathrm{P_1}(\mathrm{t}+1), \mathrm{P_2}(\mathrm{t}+1), \cdots, \mathrm{P_N}(\mathrm{t}+1)\}$.

Step 6 Calculate $\mathrm{mbest}(\mathrm{t}+1)$:

$$\mathrm{mbest}(\mathrm{t}+1) = \sum_{i=1}^{M} P_i\,(t)/M = [\sum_{i=1}^{M} P_{i1}\,(t)/M\,, \sum_{i=1}^{M} P_{i2}\,(t)/M\,, \cdots, \sum_{i=1}^{M} P_{iD}\,(t)/M].$$

Step 7 Calculate random points for each particle $\mathrm{PP}_i(t+1)$:

$$\mathrm{PP}_i(t+1) = \mathrm{J}_{mo}\big(P_i(t+1)\big)P_i(t) + [1 - \mathrm{J}_{mo}\big(P_i(t+1)\big)]P_g(t)\ .$$

Step 8 Update the new position of each particle $X_i(t+1)$:

$$X_i(t+1) = PP_i(t+1) + rand(t+1) \times a(t+1) \times |mbest(t+1) - X_i(t)|ln[1/u_i(t+1)]\ .$$

$a(t)$ is the contraction expansion coefficient of **QPSO**. $rand(t+1)$ takes - 1 and 1 respectively with a certain probability.

Step 9 If the optimization end conditions are not met, go to step 2 to continue the optimization.

5 Conclusion

Firstly, based on the unique intrinsic characteristics of **FFSR** in microgravity environment, a general **FFSR** kinematics model is established by introducing the concepts of generalized velocity, generalized force, generalized mass, generalized kinetic energy and generalized total momentum; Then, the **NCT** dynamic model based on quaternion method is established. Secondly, the joint trajectory parameterization model of **FFSR** manipulator based on sinusoidal function and the objective function of **FFSR** trajectory planning are established. Finally, considering the optimal objective function of the comprehensive index based on the minimum attitude disturbance of the satellite base and the minimum position error of the manipulator end, and meeting the constraints of the satellite base attitude variation range, joint angular velocity and angular acceleration, a **QPSO** algorithm for **FFSR** trajectory planning based on the optimal comprehensive index is proposed

The researches have been sponsored by the following scientific projects: Shenzhen basic research project (JCYJ20180307124010740), school level science and technology project (SZIIT2020KJ016,LHPY-2020007，LHPY-2020008), the seventh batch of school level education and teaching reform research and practice projects (10600-20-010201-06011).

References

1. Huang P,Wang D,MengZ,et al. Impact Dynamic Modeling and Adaptive Target Capturing Control for Tethered Space Robots with Uncertainties[J].IEEE/ASME Transactionson Mechatronics, 2016, 21(5): 2260-2271.
2. Ma G,Jiang Z, Li H, et al. Hand-eye Servo and Impedance Control for Manipulator Arm to Capture Target Satellite Safely[J]. Robotica, 2015, 33(4): 848-864.
3. Zhang L, Jia Q, Chen G, et al. Pre-impact Trajectory Planning for Minimizing Base Attitude Disturbance in Space Manipulator Systems for a Capture Task[J]. Chinese Journal of Aeronautics, 2015, 28(4): 1199-1208.
4. Dong G, Zhu Z H. Predictive Visual Servo Kinematic Control for Autonomous Robotic Capture of Non-cooperativeSpace Target[J]. ActaAstronautica, 2018.
5. Aghili, F. Coordination Control of a Free-flying Manipulator and its Base Attitude to Capture and Detumble a Non-cooperativeSatellite.Proceedings of the IEEE/RSJ International Conference on Intelligent Robots and Systems, 2009: 2365 – 2372.
6. S. Dubowsky, M.A. Torres, Path Planning for Space Manipulator to Minimize Spacecraft Attitude Disturbances. IEEE Int. C. on Robotics and Autom., Sacramento CA, 1991, pp.2522–2528.
7. E Papadopoulos， S. Dubowsky． Coordinated Manipulator / Spacecraft Motion Control for Space Robotic System s．IEEE Proc Robotics Automat April 1991:1696-1701.
8. N. Inaba and M. Oda. Autonomous Satellite Capture by a Space Robot:World First on-orbit Experiment on a Japanese Robot Satellite ETS-VII. Proc. IEEE Int. Conf. Robot. Autom., 2000:1169 – 1174.
9. M. D. Lichter and S.Dubowsky. State, Shape, and Parameter Estimation of Space Object from Range Images. Proc. IEEE Int. Conf. Robot. Autom., Apr. 2004: 2974 – 2979.
10. Z. Ma, O. Ma, and B. Shashikanth. Optimal Approach to and Alignment with a Rotating Rigid Body for Capture[J]. J. Astron. Sci., 2007，55(4): 407 – 419.

11. F. Aghili and K. Parsa. An Adaptive Vision System for Guidance of a Robotic Manipulator to Capture a Tumbling Satellite with Unknown Dynamics. Proc. IEEE/RSJ Int. Conf. Intell. Robots Syst., Nice, France, Sep. 2008: 3064–3071.
12. P. Singla, K. Subbarao, and J. L. Junkins. Adaptive Output Feedback Control for Spacecraft Rendezvous and Docking under Measurement Uncertainty [J]. AIAA J. Guid., Control, Dyn., 2006, 29(4): 892 - 902.
13. Xu W F, Li C, Wang X Q, et al. Study on Nonholonomic Cartesian Path Planning of Free Floating Space Robotic System [J]. Advanced Robotics, 2009, 23(1) :113-143.
14. LIU Zheng xiong,HUANG Pan feng,YAN Jie. Trajectory Planning of Space Manipulator Using PSO[J]. Computer Simulation [J],2010,27(11):172-175.
15. SHI Zhong, WANG Yong zhi, HU Qing lei. A Polynomial Interpolation Based Particle Swarm Optimization Algorithm for Trajectory Planning of Free-Floating Space Robot[J]. Journal of Astronautics,2011,32(7) :1516-1521.
16. SUN Jun ，FENG Bin ，XU Wenbo. Particle Swam Optimization with Particles Having Uqantum Behavior[J].Evolutionary Computation，2004，1(1):325-331.
17. Sun J, Fang W, Wu X J, et al. Quantum-Behaved Particle Swarm Optimization: Principle and Application[M].Beijing: Tsinghua University Press, 2011: 31-68.
18. Huang L, Xi M L, Sun J. Method of Trajectory Tracking Control for Mobile Robots with Improved QPSO Algorithm [J]. Computer Engineering and Applications, 2012, 48(34): 230-236.
19. SHI Ye, LIANG Bin, WANG Xueqian, XU Wenfu. Cartesian Non-holonomic Path Planning of Space Robot Based on Quantum-behaved Particle Swarm Optimization Algorithm [J]. JOURNAL OF MECHANICAL ENGINEERING, 2011, 47(23):65-73.
20. WANG Ming, HUANG Pan feng, LIU Zheng xiong, et al. Trajectory Planning for Minimizing Base Reaction of Free-Floating Space Robot[J]. Journal of Astronautics, 2011(10): 2152-2157.